BABAR-CONF-01/27
SLAC-PUB-8928
hep-ex/0107060
July, 2001

Measurement of D_s^+ and D_s^{*+} production in B meson decays and from continuum e^+e^- annihilations at $\sqrt{s} = 10.6\,\mathrm{GeV}$

The *BABAR* Collaboration

July 20, 2001

Abstract

New precise measurements of D_s^+ and D_s^{*+} meson production from B mesons and $q\overline{q}$ continuum events near the $\Upsilon(4S)$ resonance are presented in this paper. Using the *BABAR* data recorded in 1999 and 2000 of $20.8\,\mathrm{fb}^{-1}$ on-resonance and $2.6\,\mathrm{fb}^{-1}$ off-resonance, we measure the inclusive branching fractions $\mathcal{B}(B \to D_s^+ X) = (10.93 \pm 0.19 \pm 0.58 \pm 2.73)\%$ and $\mathcal{B}(B \to D_s^{*+} X) = (7.94 \pm 0.82 \pm 0.72 \pm 1.99)\%$, where the first error is statistical, the second is the systematic error, and the third is the error due to the $D_s^+ \to \phi\pi^+$ branching fraction uncertainty. The branching fractions $\Sigma\mathcal{B}(B \to D_s^{(*)+}\overline{D}^{(*)}) = (5.07 \pm 0.09 \pm 0.34 \pm 1.27)\%$ and $\Sigma\mathcal{B}(B \to D_s^{*+}\overline{D}^{(*)}) = (4.07 \pm 0.42 \pm 0.53 \pm 1.02)\%$ have been determined from the measured $D_s^{(*)+}$ momentum spectra.

Submitted to the
20th International Symposium on Lepton and Photon Interactions at High Energies,
7/23—7/28/2001, Rome, Italy

Stanford Linear Accelerator Center, Stanford University, Stanford, CA 94309

Work supported in part by Department of Energy contract DE-AC03-76SF00515.

The *BABAR* Collaboration,

B. Aubert, D. Boutigny, J.-M. Gaillard, A. Hicheur, Y. Karyotakis, J. P. Lees, P. Robbe, V. Tisserand

Laboratoire de Physique des Particules, F-74941 Annecy-le-Vieux, France

A. Palano

Università di Bari, Dipartimento di Fisica and INFN, I-70126 Bari, Italy

G. P. Chen, J. C. Chen, N. D. Qi, G. Rong, P. Wang, Y. S. Zhu

Institute of High Energy Physics, Beijing 100039, China

G. Eigen, P. L. Reinertsen, B. Stugu

University of Bergen, Inst. of Physics, N-5007 Bergen, Norway

B. Abbott, G. S. Abrams, A. W. Borgland, A. B. Breon, D. N. Brown, J. Button-Shafer, R. N. Cahn, A. R. Clark, M. S. Gill, A. V. Gritsan, Y. Groysman, R. G. Jacobsen, R. W. Kadel, J. Kadyk, L. T. Kerth, S. Kluth, Yu. G. Kolomensky, J. F. Kral, C. LeClerc, M. E. Levi, T. Liu, G. Lynch, A. B. Meyer, M. Momayezi, P. J. Oddone, A. Perazzo, M. Pripstein, N. A. Roe, A. Romosan, M. T. Ronan, V. G. Shelkov, A. V. Telnov, W. A. Wenzel

Lawrence Berkeley National Laboratory and University of California, Berkeley, CA 94720, USA

P. G. Bright-Thomas, T. J. Harrison, C. M. Hawkes, D. J. Knowles, S. W. O'Neale, R. C. Penny, A. T. Watson, N. K. Watson

University of Birmingham, Birmingham, B15 2TT, United Kingdom

T. Deppermann, K. Goetzen, H. Koch, J. Krug, M. Kunze, B. Lewandowski, K. Peters, H. Schmuecker, M. Steinke

Ruhr Universität Bochum, Institut für Experimentalphysik 1, D-44780 Bochum, Germany

J. C. Andress, N. R. Barlow, W. Bhimji, N. Chevalier, P. J. Clark, W. N. Cottingham, N. De Groot, N. Dyce, B. Foster, J. D. McFall, D. Wallom, F. F. Wilson

University of Bristol, Bristol BS8 1TL, United Kingdom

K. Abe, C. Hearty, T. S. Mattison, J. A. McKenna, D. Thiessen

University of British Columbia, Vancouver, BC, Canada V6T 1Z1

S. Jolly, A. K. McKemey, J. Tinslay

Brunel University, Uxbridge, Middlesex UB8 3PH, United Kingdom

V. E. Blinov, A. D. Bukin, D. A. Bukin, A. R. Buzykaev, V. B. Golubev, V. N. Ivanchenko, A. A. Korol, E. A. Kravchenko, A. P. Onuchin, A. A. Salnikov, S. I. Serednyakov, Yu. I. Skovpen, V. I. Telnov, A. N. Yushkov

Budker Institute of Nuclear Physics, Novosibirsk 630090, Russia

D. Best, A. J. Lankford, M. Mandelkern, S. McMahon, D. P. Stoker

University of California at Irvine, Irvine, CA 92697, USA

A. Ahsan, K. Arisaka, C. Buchanan, S. Chun

University of California at Los Angeles, Los Angeles, CA 90024, USA

J. G. Branson, D. B. MacFarlane, S. Prell, Sh. Rahatlou, G. Raven, V. Sharma

University of California at San Diego, La Jolla, CA 92093, USA

C. Campagnari, B. Dahmes, P. A. Hart, N. Kuznetsova, S. L. Levy, O. Long, A. Lu, J. D. Richman, W. Verkerke, M. Witherell, S. Yellin

University of California at Santa Barbara, Santa Barbara, CA 93106, USA

J. Beringer, D. E. Dorfan, A. M. Eisner, A. Frey, A. A. Grillo, M. Grothe, C. A. Heusch, R. P. Johnson, W. Kroeger, W. S. Lockman, T. Pulliam, H. Sadrozinski, T. Schalk, R. E. Schmitz, B. A. Schumm, A. Seiden, M. Turri, W. Walkowiak, D. C. Williams, M. G. Wilson

University of California at Santa Cruz, Institute for Particle Physics, Santa Cruz, CA 95064, USA

E. Chen, G. P. Dubois-Felsmann, A. Dvoretskii, D. G. Hitlin, S. Metzler, J. Oyang, F. C. Porter, A. Ryd, A. Samuel, M. Weaver, S. Yang, R. Y. Zhu

California Institute of Technology, Pasadena, CA 91125, USA

S. Devmal, T. L. Geld, S. Jayatilleke, G. Mancinelli, B. T. Meadows, M. D. Sokoloff

University of Cincinnati, Cincinnati, OH 45221, USA

T. Barillari, P. Bloom, M. O. Dima, S. Fahey, W. T. Ford, D. R. Johnson, U. Nauenberg, A. Olivas, H. Park, P. Rankin, J. Roy, S. Sen, J. G. Smith, W. C. van Hoek, D. L. Wagner

University of Colorado, Boulder, CO 80309, USA

J. Blouw, J. L. Harton, M. Krishnamurthy, A. Soffer, W. H. Toki, R. J. Wilson, J. Zhang

Colorado State University, Fort Collins, CO 80523, USA

T. Brandt, J. Brose, T. Colberg, G. Dahlinger, M. Dickopp, R. S. Dubitzky, A. Hauke, E. Maly, R. Müller-Pfefferkorn, S. Otto, K. R. Schubert, R. Schwierz, B. Spaan, L. Wilden

Technische Universität Dresden, Institut für Kern- und Teilchenphysik, D-01062, Dresden, Germany

L. Behr, D. Bernard, G. R. Bonneaud, F. Brochard, J. Cohen-Tanugi, S. Ferrag, E. Roussot, S. T'Jampens, Ch. Thiebaux, G. Vasileiadis, M. Verderi

Ecole Polytechnique, F-91128 Palaiseau, France

A. Anjomshoaa, R. Bernet, A. Khan, D. Lavin, F. Muheim, S. Playfer, J. E. Swain

University of Edinburgh, Edinburgh EH9 3JZ, United Kingdom

M. Falbo

Elon University, Elon University, NC 27244-2010, USA

C. Borean, C. Bozzi, S. Dittongo, M. Folegani, L. Piemontese

Università di Ferrara, Dipartimento di Fisica and INFN, I-44100 Ferrara, Italy

E. Treadwell

Florida A&M University, Tallahassee, FL 32307, USA

F. Anulli,[1] R. Baldini-Ferroli, A. Calcaterra, R. de Sangro, D. Falciai, G. Finocchiaro, P. Patteri, I. M. Peruzzi,[2]1 M. Piccolo, Y. Xie, A. Zallo

Laboratori Nazionali di Frascati dell'INFN, I-00044 Frascati, Italy

[1]Also with Università di Perugia, I-06100 Perugia, Italy

S. Bagnasco, A. Buzzo, R. Contri, G. Crosetti, P. Fabbricatore, S. Farinon, M. Lo Vetere, M. Macri, M. R. Monge, R. Musenich, M. Pallavicini, R. Parodi, S. Passaggio, F. C. Pastore, C. Patrignani, M. G. Pia, C. Priano, E. Robutti, A. Santroni

Università di Genova, Dipartimento di Fisica and INFN, I-16146 Genova, Italy

M. Morii

Harvard University, Cambridge, MA 02138, USA

R. Bartoldus, T. Dignan, R. Hamilton, U. Mallik

University of Iowa, Iowa City, IA 52242, USA

J. Cochran, H. B. Crawley, P.-A. Fischer, J. Lamsa, W. T. Meyer, E. I. Rosenberg

Iowa State University, Ames, IA 50011-3160, USA

M. Benkebil, G. Grosdidier, C. Hast, A. Höcker, H. M. Lacker, S. Laplace, V. Lepeltier, A. M. Lutz, S. Plaszczynski, M. H. Schune, S. Trincaz-Duvoid, A. Valassi, G. Wormser

Laboratoire de l'Accélérateur Linéaire, F-91898 Orsay, France

R. M. Bionta, V. Brigljević , D. J. Lange, M. Mugge, X. Shi, K. van Bibber, T. J. Wenaus, D. M. Wright, C. R. Wuest

Lawrence Livermore National Laboratory, Livermore, CA 94550, USA

M. Carroll, J. R. Fry, E. Gabathuler, R. Gamet, M. George, M. Kay, D. J. Payne, R. J. Sloane, C. Touramanis

University of Liverpool, Liverpool L69 3BX, United Kingdom

M. L. Aspinwall, D. A. Bowerman, P. D. Dauncey, U. Egede, I. Eschrich, N. J. W. Gunawardane, J. A. Nash, P. Sanders, D. Smith

University of London, Imperial College, London, SW7 2BW, United Kingdom

D. E. Azzopardi, J. J. Back, P. Dixon, P. F. Harrison, R. J. L. Potter, H. W. Shorthouse, P. Strother, P. B. Vidal, M. I. Williams

Queen Mary, University of London, E1 4NS, United Kingdom

G. Cowan, S. George, M. G. Green, A. Kurup, C. E. Marker, P. McGrath, T. R. McMahon, S. Ricciardi, F. Salvatore, I. Scott, G. Vaitsas

University of London, Royal Holloway and Bedford New College, Egham, Surrey TW20 0EX, United Kingdom

D. Brown, C. L. Davis

University of Louisville, Louisville, KY 40292, USA

J. Allison, R. J. Barlow, J. T. Boyd, A. C. Forti, J. Fullwood, F. Jackson, G. D. Lafferty, N. Savvas, E. T. Simopoulos, J. H. Weatherall

University of Manchester, Manchester M13 9PL, United Kingdom

A. Farbin, A. Jawahery, V. Lillard, J. Olsen, D. A. Roberts, J. R. Schieck

University of Maryland, College Park, MD 20742, USA

G. Blaylock, C. Dallapiccola, K. T. Flood, S. S. Hertzbach, R. Kofler, T. B. Moore, H. Staengle, S. Willocq

University of Massachusetts, Amherst, MA 01003, USA

B. Brau, R. Cowan, G. Sciolla, F. Taylor, R. K. Yamamoto
Massachusetts Institute of Technology, Laboratory for Nuclear Science, Cambridge, MA 02139, USA

M. Milek, P. M. Patel, J. Trischuk
McGill University, Montréal, Canada QC H3A 2T8

F. Lanni, F. Palombo
Università di Milano, Dipartimento di Fisica and INFN, I-20133 Milano, Italy

J. M. Bauer, M. Booke, L. Cremaldi, V. Eschenburg, R. Kroeger, J. Reidy, D. A. Sanders, D. J. Summers
University of Mississippi, University, MS 38677, USA

J. P. Martin, J. Y. Nief, R. Seitz, P. Taras, A. Woch, V. Zacek
Université de Montréal, Laboratoire René J. A. Lévesque, Montréal, Canada QC H3C 3J7

H. Nicholson, C. S. Sutton
Mount Holyoke College, South Hadley, MA 01075, USA

C. Cartaro, N. Cavallo,[3] G. De Nardo, F. Fabozzi, C. Gatto, L. Lista, P. Paolucci, D. Piccolo, C. Sciacca
Università di Napoli Federico II, Dipartimento di Scienze Fisiche and INFN, I-80126, Napoli, Italy

J. M. LoSecco
University of Notre Dame, Notre Dame, IN 46556, USA

J. R. G. Alsmiller, T. A. Gabriel, T. Handler
Oak Ridge National Laboratory, Oak Ridge, TN 37831, USA

J. Brau, R. Frey, M. Iwasaki, N. B. Sinev, D. Strom
University of Oregon, Eugene, OR 97403, USA

F. Colecchia, F. Dal Corso, A. Dorigo, F. Galeazzi, M. Margoni, G. Michelon, M. Morandin, M. Posocco, M. Rotondo, F. Simonetto, R. Stroili, E. Torassa, C. Voci
Università di Padova, Dipartimento di Fisica and INFN, I-35131 Padova, Italy

M. Benayoun, H. Briand, J. Chauveau, P. David, Ch. de la Vaissière, L. Del Buono, O. Hamon, F. Le Diberder, Ph. Leruste, J. Lory, L. Roos, J. Stark, S. Versillé
Universités Paris VI et VII, Lab de Physique Nucléaire H. E., F-75252 Paris, France

P. F. Manfredi, V. Re, V. Speziali
Università di Pavia, Dipartimento di Elettronica and INFN, I-27100 Pavia, Italy

E. D. Frank, L. Gladney, Q. H. Guo, J. H. Panetta
University of Pennsylvania, Philadelphia, PA 19104, USA

C. Angelini, G. Batignani, S. Bettarini, M. Bondioli, M. Carpinelli, F. Forti, M. A. Giorgi, A. Lusiani, F. Martinez-Vidal, M. Morganti, N. Neri, E. Paoloni, M. Rama, G. Rizzo, F. Sandrelli, G. Simi, G. Triggiani, J. Walsh
Università di Pisa, Scuola Normale Superiore and INFN, I-56010 Pisa, Italy

[3]Also with Università della Basilicata, I-85100 Potenza, Italy

M. Haire, D. Judd, K. Paick, L. Turnbull, D. E. Wagoner

Prairie View A&M University, Prairie View, TX 77446, USA

J. Albert, C. Bula, P. Elmer, C. Lu, K. T. McDonald, V. Miftakov, S. F. Schaffner, A. J. S. Smith, A. Tumanov, E. W. Varnes

Princeton University, Princeton, NJ 08544, USA

G. Cavoto, D. del Re, R. Faccini,[4] F. Ferrarotto, F. Ferroni, K. Fratini, E. Lamanna, E. Leonardi, M. A. Mazzoni, S. Morganti, G. Piredda, F. Safai Tehrani, M. Serra, C. Voena

Università di Roma La Sapienza, Dipartimento di Fisica and INFN, I-00185 Roma, Italy

S. Christ, R. Waldi

Universität Rostock, D-18051 Rostock, Germany

P. F. Jacques, M. Kalelkar, R. J. Plano

Rutgers University, New Brunswick, NJ 08903, USA

T. Adye, B. Franek, N. I. Geddes, G. P. Gopal, S. M. Xella

Rutherford Appleton Laboratory, Chilton, Didcot, Oxon, OX11 0QX, United Kingdom

R. Aleksan, G. De Domenico, S. Emery, A. Gaidot, S. F. Ganzhur, P.-F. Giraud, G. Hamel de Monchenault, W. Kozanecki, M. Langer, G. W. London, B. Mayer, B. Serfass, G. Vasseur, Ch. Yèche, M. Zito

DAPNIA, Commissariat à l'Energie Atomique/Saclay, F-91191 Gif-sur-Yvette, France

N. Copty, M. V. Purohit, H. Singh, F. X. Yumiceva

University of South Carolina, Columbia, SC 29208, USA

I. Adam, P. L. Anthony, D. Aston, K. Baird, J. P. Berger, E. Bloom, A. M. Boyarski, F. Bulos, G. Calderini, R. Claus, M. R. Convery, D. P. Coupal, D. H. Coward, J. Dorfan, M. Doser, W. Dunwoodie, R. C. Field, T. Glanzman, G. L. Godfrey, S. J. Gowdy, P. Grosso, T. Himel, T. Hryn'ova, M. E. Huffer, W. R. Innes, C. P. Jessop, M. H. Kelsey, P. Kim, M. L. Kocian, U. Langenegger, D. W. G. S. Leith, S. Luitz, V. Luth, H. L. Lynch, H. Marsiske, S. Menke, R. Messner, K. C. Moffeit, R. Mount, D. R. Muller, C. P. O'Grady, M. Perl, S. Petrak, H. Quinn, B. N. Ratcliff, S. H. Robertson, L. S. Rochester, A. Roodman, T. Schietinger, R. H. Schindler, J. Schwiening, V. V. Serbo, A. Snyder, A. Soha, S. M. Spanier, J. Stelzer, D. Su, M. K. Sullivan, H. A. Tanaka, J. Va'vra, S. R. Wagner, A. J. R. Weinstein, W. J. Wisniewski, D. H. Wright, C. C. Young

Stanford Linear Accelerator Center, Stanford, CA 94309, USA

P. R. Burchat, C. H. Cheng, D. Kirkby, T. I. Meyer, C. Roat

Stanford University, Stanford, CA 94305-4060, USA

R. Henderson

TRIUMF, Vancouver, BC, Canada V6T 2A3

W. Bugg, H. Cohn, A. W. Weidemann

University of Tennessee, Knoxville, TN 37996, USA

[4]Also with University of California at San Diego, La Jolla, CA 92093, USA

J. M. Izen, I. Kitayama, X. C. Lou, M. Turcotte
University of Texas at Dallas, Richardson, TX 75083, USA

F. Bianchi, M. Bona, B. Di Girolamo, D. Gamba, A. Smol, D. Zanin
Università di Torino, Dipartimento di Fisica Sperimentale and INFN, I-10125 Torino, Italy

L. Bosisio, G. Della Ricca, L. Lanceri, A. Pompili, P. Poropat, M. Prest, E. Vallazza, G. Vuagnin
Università di Trieste, Dipartimento di Fisica and INFN, I-34127 Trieste, Italy

R. S. Panvini
Vanderbilt University, Nashville, TN 37235, USA

C. M. Brown, A. De Silva, R. Kowalewski, J. M. Roney
University of Victoria, Victoria, BC, Canada V8W 3P6

H. R. Band, E. Charles, S. Dasu, F. Di Lodovico, A. M. Eichenbaum, H. Hu, J. R. Johnson, R. Liu, J. Nielsen, Y. Pan, R. Prepost, I. J. Scott, S. J. Sekula, J. H. von Wimmersperg-Toeller, S. L. Wu, Z. Yu, H. Zobernig
University of Wisconsin, Madison, WI 53706, USA

T. M. B. Kordich, H. Neal
Yale University, New Haven, CT 06511, USA

1 Introduction

The study of $D_s^{(*)+}$ meson production in B decays allows exploration of the mechanisms leading to the creation of $c\overline{s}$ quark pairs. Although several Feynman diagrams could lead to $D_s^{(*)+}$ mesons in B decays, the spectator diagram (Fig. 1) is expected to dominate. In addition, $D_s^{(*)+}$ mesons could be produced from $c\overline{c}$ continuum events. It has been pointed out [1] that the rate from B decays may be large. This might help to explain some of the theoretical difficulties [2] in accounting simultaneously for the total inclusive B decay rate and the semileptonic branching fraction of the B meson. The measurement of the $D_s^{(*)+}$ momentum allows a determination of the fraction of two-body and multi-body decay modes, which will aid understanding $b \to c\overline{c}s$ transitions.

In this paper, measurements of $B \to D_s^+ X$ and $B \to D_s^{*+} X$ production rates and momentum spectra[1] are presented. These mesons are reconstructed using the decays $D_s^+ \to \phi\pi^+$ and $D_s^{*+} \to D_s^+\gamma$.

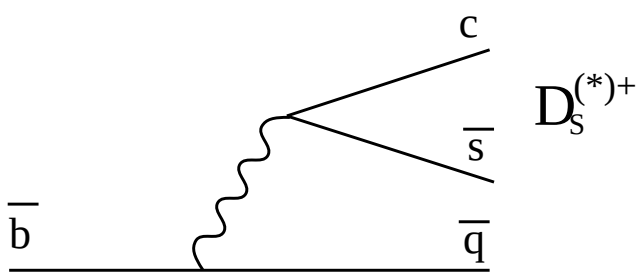

Figure 1: The main spectator diagram leading to the production of $D_s^{(*)+}$ mesons in B decays.

2 The *BABAR* detector and data set

The data used for this analysis were collected with the *BABAR* detector [3] at the PEP-II asymmetric-energy collider [4] at the Stanford Linear Accelerator center. An integrated luminosity of 20.8 fb^{-1} was recorded corresponding to about 22.7 million produced $B\overline{B}$ pairs at the $\Upsilon(4S)$ resonance ("on-resonance") and 2.6 fb^{-1} at an energy about 40 MeV below the $B\overline{B}$ threshold ("off-resonance"). Since a detailed description of the *BABAR* detector is presented in Ref. [3], only the components of the detector most crucial to this analysis are briefly summarized below.

Charged particles are detected and their momenta measured by a combination of a central drift chamber (DCH) with a helium-based gas and a five-layer (double-sided) silicon vertex tracker (SVT), within a 1.5 T solenoidal field produced by a superconducting magnet. The tracking system covers a solid angle of 92% in the center-of-mass frame. Charged particles are identified using the ionization energy loss ($\mathrm{d}E/\mathrm{d}x$) measured in the DCH and SVT and the Cherenkov radiation detected in a ring imaging Cherenkov device (DIRC). Photons are identified by the CsI electromagnetic calorimeter.

[1] Reference in this paper to a specific decay channel or state also implies the charge conjugated decay or state. The notation $D_s^{(*)+}$ means either D_s^+ or D_s^{*+}. $B \to D_s^{(*)+}\overline{D}^{(*)}$ is a general representation of any of modes with $c\overline{s}$, $\overline{c}q$ including their excited states.

3 D_s^+ and D_s^{*+} selection

The analysis reported here uses only the decay mode $D_s^+ \to \phi\pi^+$, with $\phi \to K^+K^-$, as this channel offers the best signal-to-background ratio. The charged tracks are required to originate from within ± 10 cm along the beam direction and ± 1.5 cm in the transverse plane of the interaction point and leave at least 12 hits in the drift chamber.

In order to obtain a sufficiently clean sample, kaon identification is required for the tracks forming the ϕ meson by using $\mathrm{d}E/\mathrm{d}x$ information from DCH and SVT and the Cherenkov angle and the number of photons as measured by the DIRC. The kaon selection is based on the likelihoods given by each detector and uses, for each track, the ratio of likelihoods for the pion and the kaon mass hypotheses, L_π/L_K. If this ratio is less than unity for at least one of the considered subsystems, the particle is selected as a kaon. The DIRC is used both in a positive identification mode and also in a veto mode for the case where a kaon with the measured track momentum would not be above the Cherenkov threshold. A tighter level of identification is also available using a total likelihood defined as the product of the likelihoods of each subsystem. In this case the track is tagged as a kaon if the ratio of the total likelihoods for the pion and kaon mass hypotheses is less than unity.

Three charged tracks originating from a common vertex are combined to form a D_s^+ candidate. Two oppositely charged tracks have to be identified as kaons by satisfying the basic criteria and at least one of them has to satisfy the tighter selection. The K^+K^- invariant mass must be within $8\,\mathrm{MeV}/c^2$ of the nominal ϕ mass [5]. In this particular decay, the ϕ meson is polarized longitudinally and therefore the angular distribution of the kaons has a $\cos^2\theta_H$ dependence, where θ_H is the angle between the K^+ and D_s^+ in the ϕ rest frame. This angle is required to satisfy $|\cos\theta_H| > 0.3$, thereby keeping 97.5% of the signal while rejecting about 30% of the background.

Using the selection described above, a clean D_s^+ signal of 47794 ± 311 events is observed (Fig. 2). A clear signal for the Cabibbo-suppressed decay mode $D^+ \to \phi\pi^+$ is also observed.

D_s^{*+} mesons are reconstructed using the decay $D_s^{*+} \to D_s^+\gamma$, with the subsequent decay $D_s^+ \to \phi\pi^+$. D_s^+ candidates are selected by requiring the $\phi\pi$ invariant mass to be within 2.5 standard deviations (σ) of the peak value. These are then combined with the "single photons" of the event, which are required to satisfy $E_\gamma > 50\,\mathrm{MeV}$, where E_γ is the photon energy in the laboratory frame, and $E_\gamma^* > 110\,\mathrm{MeV}$, where E_γ^* is the photon energy in the $\Upsilon(4S)$ rest frame. In order to reduce the combinatoric background, the candidate photon should not form a π^0, defined by a total energy $E_{\gamma\gamma}^* > 200\,\mathrm{MeV}$ and an invariant mass $115 < M_{\gamma\gamma} < 155\,\mathrm{MeV}/c^2$, when combined with any other photon in the event. The distribution of the mass difference $\Delta M = M_{D_s^+\gamma} - M_{D_s^+}$ is shown in Fig. 3. A clear peak with 14392 ± 376 events is observed.

4 Extraction of the $D_s^{(*)+}$ momentum spectra

The momentum spectrum of D_s^+ mesons in the $\Upsilon(4S)$ rest frame is extracted by fitting the $\phi\pi$ invariant mass distribution in each momentum bin. The bins are chosen to be $200\,\mathrm{MeV}/c$ wide, which is much larger than the momentum resolution ($\approx 6\,\mathrm{MeV}/c$). The fit function is a single Gaussian for each of the D_s^+ and the D^+ signals, with the constraint of a common width. The combinatorial background is accounted for by an exponential. As there are many more events for the on-resonance data, the number of D_s^+ in the off-resonance data is extracted with the same fit function but with M_{D^+}, $M_{D_s^+}$ and σ fixed to the values obtained from the binned chi-squared fit to the on-resonance data.

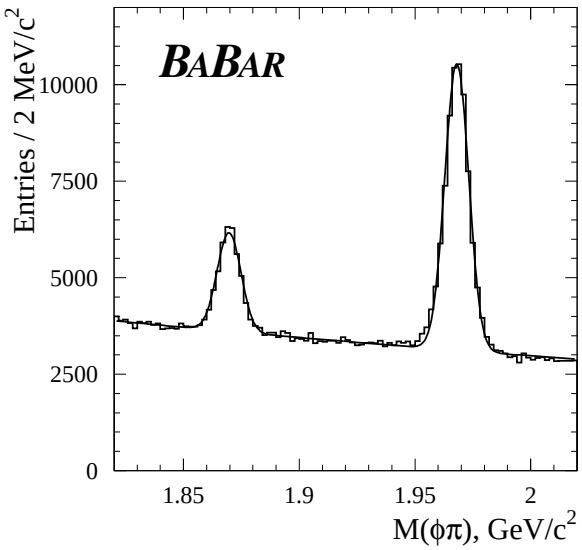

Figure 2: The observed $\phi\pi$ invariant mass spectrum. The lower mass peak corresponds to the Cabibbo-suppressed decay mode $D^+ \to \phi\pi^+$. The fit function is a single Gaussian for each peak, with their widths constrained to be equal, on top of an exponential background.

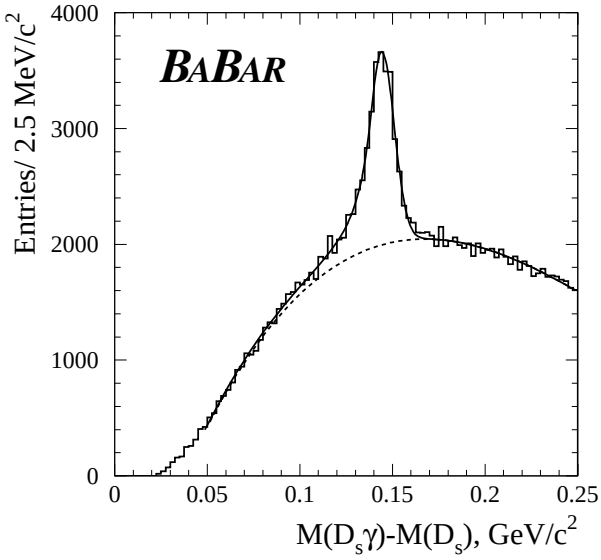

Figure 3: Distribution of the $\Delta M = M_{D_s^+\gamma} - M_{D_s^+}$ mass difference. The fit function is a Crystal Ball function for the signal on top of a threshold function, as described in text.

In the same way as for D_s^+, the momentum spectrum of D_s^{*+} mesons in the $\Upsilon(4S)$ rest frame is extracted by fitting the ΔM invariant mass distribution for $250\,\mathrm{MeV}/c$ wide momentum bins. The ΔM distribution for the signal is characterized by an asymmetric shape to account for energy leakage and shower shape fluctuations. The fit function for the signal is the Crystal Ball function [6]. For the background, a threshold function

$$f(\Delta M) = p_1(\Delta M - p_2)^{p_3} e^{p_4(\Delta M - p_2)}$$

is used, with the four free parameters p_i being determined from the fit. After ensuring that the connection point between the Gaussian and power-law tail of the Crystal Ball function does not depend on momentum and agrees with the Monte Carlo, this parameter has been fixed at 0.89σ in the final fit. The off-resonance data are again fit with the signal shape parameters ΔM and σ fixed to the values obtained from the fit to the on-resonance data.

The uncertainty on the shape of the background leads to an additional systematic error. This error is estimated by using different parameterizations for the background shape.

The efficiency obtained from Monte Carlo with generic $B\overline{B}$ and $c\overline{c}$ events varies as a function of the $D_s^{(*)+}$ momentum (p^*) in the $\Upsilon(4S)$ rest frame and ranges from 20% when the D_s^+ is at rest to 40% for $p^* = 5\,\mathrm{GeV}/c$, and from 5% to 20% for D_s^{*+}. The number of reconstructed D_s^+ and D_s^{*+} is corrected bin-by-bin for the efficiency. The efficiency-corrected number of D_s^+ and D_s^{*+} as a function of their momentum in the $\Upsilon(4S)$ rest frame is shown in Fig. 4.

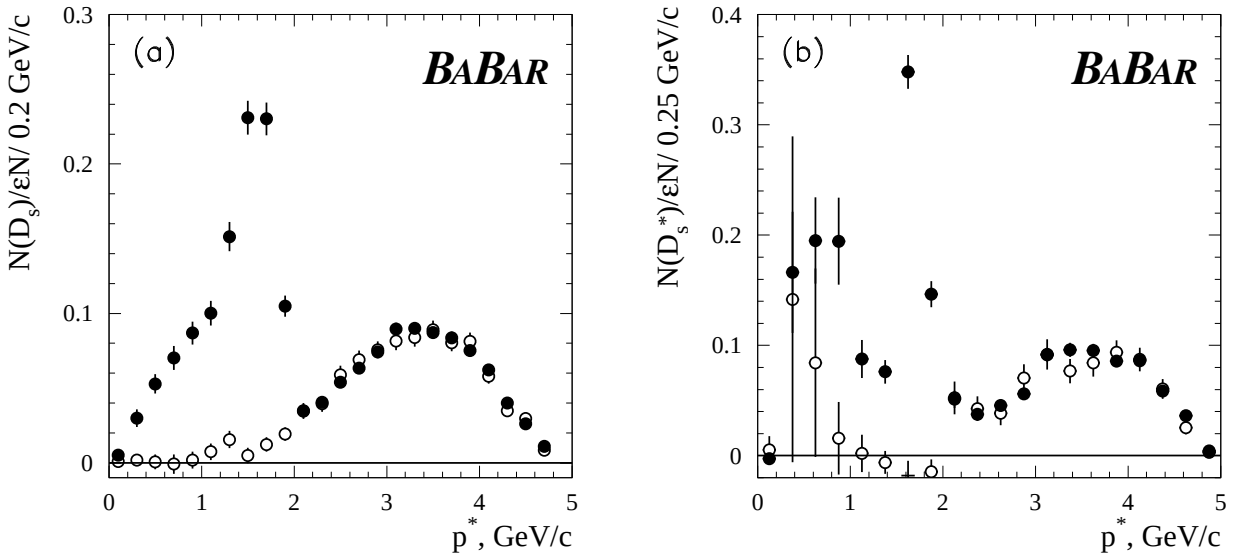

Figure 4: The (a) D_s^+ and (b) D_s^{*+} efficiency-corrected momentum spectra for on-resonance data (solid circles) and for scaled off-resonance data (open circles).

5 Branching fractions

The D_s^+ and D_s^{*+} cross sections for production from the $q\overline{q}$ continuum are obtained by integrating the spectrum obtained from the off-resonance data. This gives the preliminary results

$$\sigma(e^+e^- \to D_s^{\pm}X) \times \mathcal{B}(D_s^+ \to \phi\pi^+) = 7.55 \pm 0.20 \pm 0.34 \text{ pb}$$

and

$$\sigma(e^+e^- \to D_s^{*\pm}X) \times \mathcal{B}(D_s^+ \to \phi\pi^+) = 5.79 \pm 0.66 \pm 0.50 \text{ pb}.$$

The off-resonance data are scaled according to the luminosity ratio and then subtracted bin-by-bin from the on-resonance data in order to find the $D_s^{(*)+}$ momentum spectra from B meson decays. It is important to note that, with this method, the result is independent of any assumption about the shape of the fragmentation function, and most of the systematic errors due to the background parameterization cancel. Integrating the spectrum after continuum subtraction gives a total D_s^+ yield from B meson decays of 87711±1485. This corresponds to the inclusive preliminary branching fraction

$$\mathcal{B}(B \to D_s^+X) = \left[(10.93 \pm 0.19 \pm 0.58) \times \frac{3.6 \pm 0.9\%}{\mathcal{B}(D_s^+ \to \phi\pi^+)}\right]\%.$$

The total D_s^{*+} yield from B meson decays is 60047±6201 events, leading to the inclusive preliminary branching fraction

$$\mathcal{B}(B \to D_s^{*+}X) = \left[(7.94 \pm 0.82 \pm 0.72) \times \frac{3.6 \pm 0.9\%}{\mathcal{B}(D_s^+ \to \phi\pi^+)}\right]\%.$$

In the results above, the first error is statistical, the second is the systematic error and the third error, which is dominant, is due to the uncertainty in the $D_s^+ \to \phi\pi^+$ branching fraction [5]. The

Table 1: Systematic errors for $\mathcal{B}(B \to D_s^{(*)+} X)$

Source	Fractional Error on $\mathcal{B}$ (%)	
	$B \to D_s^+ X$	$B \to D_s^{*+} X$
Signal shape	0.5	3.0
Background parameterization	0.4	4.2
Monte Carlo statistics	2.5	4.2
Bin width	1.4	2.0
Total for D_s^+ yield	2.9	7.0
Number of $B\overline{B}$ events	1.6	1.6
$\mathcal{B}(\phi \to K^+K^-)$	1.6	1.6
Particle id efficiency	1.0	1.0
Tracking efficiency	3.6	3.6
$\mathcal{B}(D_s^{*+} \to D_s^+\gamma)$		2.7
Photon efficiency		1.3
π^0 veto		2.7
Total systematic error	5.3	9.0

various contributions to the systematic error are listed in Table 1. One of the dominant systematic errors is the 3.6% total uncertainty due to our knowledge of the tracking efficiency (1.2% per track for the decay chain $D_s^+ \to \phi\pi^+$, $\phi \to K^+K^-$).

6 Fits to $D_s^{(*)+}$ momentum spectra

In the $\Upsilon(4S)$ rest frame, two-body B decays produce $D_s^{(*)+}$ mesons with a flat momentum spectrum over a 300 MeV/c wide range. In B decays, the $D_s^{(*)+}$ momentum spectrum is essentially governed by the production of direct $D_s^{(*)+}$. Other $c\overline{s}$ states such as $D_{s1}(2536)$ and $D_{s2}^*(2573)$ primarily decay to $D^{(*)}K$. Because D_s^{*+} decays to $D_s^+\gamma$ or $D_s^+\pi^0$, the D_s^+ momentum distribution is slightly broader and shifted downward compared to direct production from $B \to D_s^+ X$.

In fitting the observed momentum spectra, three different sources of $D_s^{(*)+}$ mesons in B decays are considered:

(1) $B \to D_s^{(*)+}\overline{D}^{(*)}$ decays. The relative branching fractions of the individual channels can be taken either from existing measurements [7] or from predictions assuming factorization [8, 9, 10]. The fit is performed for both cases, with the assumption $f_{D_s^{*+}} = f_{D_s^+}$ for the theoretical models, where $f_{D_s^{(*)+}}$ are the $D_s^{(*)+}$ decay constants.

(2) $B \to D_s^{(*)+}\overline{D}^{**}$ decays. The contributions from $B \to D_s^{(*)+}\overline{D}_0^*(j = 1/2)$, $B \to D_s^{(*)+}\overline{D}_1(2420)$, $B \to D_s^{(*)+}\overline{D}_1(j = 1/2)$ and $B \to D_s^{(*)+}\overline{D}_2^*(2460)$ are included in this source.

(3) Three-body $B \to D_s^{(*)+}\overline{D}^{(*)}\pi/\rho/\omega$ decays. Since little is known on these decays, they are attributed an equal weight and the momentum distributions are generated according to phase space.

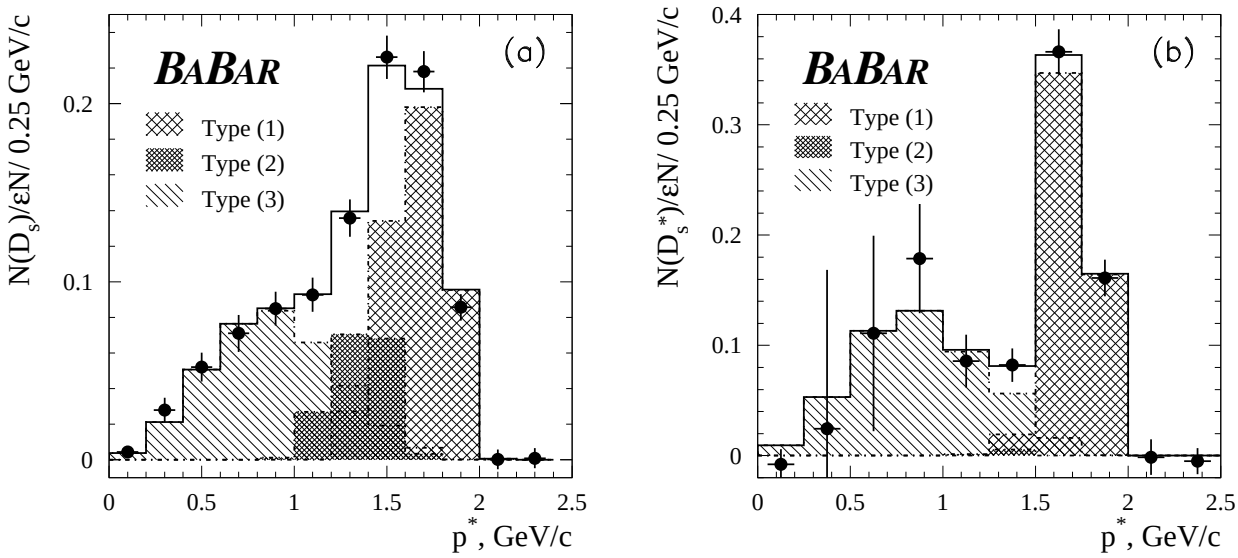

Figure 5: The fit result for (a) D_s^+ and (b) $D_s^{(*)+}$ momentum spectra. The data are dots with error bars, the histograms are the components of the fit function described in the text. Type (1) is $B \to D_s^{(*)+}\overline{D}^{(*)}$, Type (2) is $B \to D_s^{(*)+}\overline{D}^{**}$ and Type (3) is $B \to D_s^{(*)+}\overline{D}^{(*)}\pi/\rho/\omega$. The solid histogram is the sum of three components.

As a result of a chi-squared fit of D_s^+ momentum spectrum with these components, the ratio of two-body modes to the total inclusive rate is determined to be

$$\frac{\Sigma\mathcal{B}(B \to D_s^{(*)+}\overline{D}^{(*)})}{\mathcal{B}(B \to D_s^+ X)} = (46.4 \pm 1.9 \pm 0.6)\%,$$

where the first error is statistical and the second is due to model uncertainty. This last is obtained from the variation of the fit result with different individual contributions from the modes included with each of the three sources of D_s^+ mesons, as discussed below. From the fit to the D_s^{*+} momentum spectrum, we find

$$\frac{\Sigma\mathcal{B}(B \to D_s^{*+}\overline{D}^{(*)})}{\mathcal{B}(B \to D_s^{*+} X)} = (53.3 \pm 4.5 \pm 1.6 \pm 2.1)\%.$$

where the first error is statistical, the second error represents the systematic uncertainty due to the background parameterization (negligible for $B \to D_s^{(*)+}\overline{D}^{(*)}$), and the third error is due to model uncertainty obtained as for $B \to D_s^{(*)+}\overline{D}^{(*)}$.

The fit is performed under different assumptions for the relative contributions of the modes in source (1), varied according to the theoretical predictions and measurements. Different weights of $B \to D_s^+\overline{D}^{**}$ and $B \to D_s^{*+}\overline{D}^{**}$, as well as different relative branching fractions of the four modes within source (2), are also used. In source (3), two cases are considered: either $B \to D_s^{(*)}\overline{D}^{(*)}\pi$ or $B \to D_s^{(*)}\overline{D}^{(*)}\rho/\omega$ is assumed to be dominant. The best χ^2 for the fit to the inclusive D_s^{*+} momentum spectrum is obtained when the contribution from $B \to D_s^{(*)}\overline{D}^{(*)}\rho/\omega$ is dominant

compared to $B \to D_s^{(*)} \overline{D}^{(*)} \pi$. The results of the fits to the $D_s^{(*)+}$ momentum spectra are shown in Fig. 5 for one of the assumptions.

Using the fit results and the relative rates for $B \to D_s^{(*)} \overline{D}^{(*)}$ we find the preliminary results

$$\Sigma\mathcal{B}(B \to D_s^{(*)+} \overline{D}^{(*)}) = (5.07 \pm 0.09 \pm 0.34 \pm 1.27)\%,$$

$$\Sigma\mathcal{B}(B \to D_s^{*+} \overline{D}^{(*)}) = (4.07 \pm 0.42 \pm 0.53 \pm 1.02)\%.$$

where the errors from the fits to the momentum spectra are added in quadrature with the systematic error due to the $D_s^+ \to \phi\pi^+$ branching fraction uncertainty.

7 Summary

In summary, preliminary branching fractions for inclusive $B \to D_s^{(*)+} X$ production have been determined to be $\mathcal{B}(B \to D_s^+ X) = (10.93 \pm 0.19 \pm 0.58 \pm 2.73)\%$ and $\mathcal{B}(B \to D_s^{*+} X) = (7.94 \pm 0.82 \pm 0.72 \pm 1.99)\%$. The $D_s^{(*)+}$ cross sections from $q\overline{q}$ continuum events at about 40 MeV below $\Upsilon(4S)$ mass are $\sigma(e^+e^- \to D_s^{\pm} X) \times \mathcal{B}(D_s^+ \to \phi\pi^+) = 7.55 \pm 0.20 \pm 0.34$ pb and $\sigma(e^+e^- \to D_s^{*\pm} X) \times \mathcal{B}(D_s^+ \to \phi\pi^+) = 5.79 \pm 0.66 \pm 0.50$ pb. Our results for D_s^+ are in agreement with previous measurements [7, 11], although with considerable improvement in accuracy. In contrast to previous measurements, our results do not rely on any assumptions concerning the shape of the fragmentation function.

From a fit to the $D_s^{(*)+}$ momentum spectra, preliminary results have been obtained for the fraction of all two-body $B \to D_s^{(*)+} \overline{D}^{(*)}$ decays relative to the total inclusive D_s^+ yield $(46.4 \pm 1.9 \pm 0.6)\%$ and for all $B \to D_s^{*+} \overline{D}^{(*)}$ decays relative to the total inclusive D_s^{*+} yield $(53.3 \pm 4.5 \pm 1.6 \pm 2.1)\%$, where the last error includes the model dependence. Combining these results gives $\Sigma\mathcal{B}(B \to D_s^{(*)+} \overline{D}^{(*)}) = (5.07 \pm 0.09 \pm 0.34 \pm 1.27)\%$ and $\Sigma\mathcal{B}(B \to D_s^{*+} \overline{D}^{(*)}) = (4.07 \pm 0.42 \pm 0.53 \pm 1.02)\%$

8 Acknowledgements

We are grateful for the extraordinary contributions of our PEP-II colleagues in achieving the excellent luminosity and machine conditions that have made this work possible. The collaborating institutions wish to thank SLAC for its support and the kind hospitality extended to them. This work is supported by the US Department of Energy and National Science Foundation, the Natural Sciences and Engineering Research Council (Canada), Institute of High Energy Physics (China), the Commissariat à l'Energie Atomique and Institut National de Physique Nucléaire et de Physique des Particules (France), the Bundesministerium für Bildung und Forschung (Germany), the Istituto Nazionale di Fisica Nucleare (Italy), the Research Council of Norway, the Ministry of Science and Technology of the Russian Federation, and the Particle Physics and Astronomy Research Council (United Kingdom). Individuals have received support from the Swiss National Science Foundation, the A. P. Sloan Foundation, the Research Corporation, and the Alexander von Humboldt Foundation.

References

[1] A. F. Falk, M. B. Wise and I. Dunietz, Phys. Rev. D **51**, 1183-1191 (1995).

[2] I. Bigi *et al.*, Phys. Lett. B **323**, 408-416 (1994).

[3] *BABAR* Collaboration, B. Aubert *et al.*, SLAC-PUB-8569, hep-ex/0105044, to appear in Nucl. Instrum. and Methods.

[4] PEP-II Conceptual Design Report, SLAC-R-418 (1993).

[5] Particle Data Group, D. E. Groom *et al.*, Eur. Phys. Jour. C **15**, 1 (2000).

[6] The ΔM distribution for the $D_s^+\gamma$ signal is fit with the Crystal Ball function

$$f(x) = N \cdot \begin{cases} \exp(-\frac{(x-\bar{x})^2}{2\,\sigma^2}) & ;(x-\bar{x})/\sigma > \alpha \\ A \times (B - \frac{x-\bar{x}}{\sigma})^{-n} & ;(x-\bar{x})/\sigma \leq \alpha \end{cases}$$

where $A \equiv \left(\frac{n}{|\alpha|}\right)^n \times \exp(-|\alpha|^2/2)$ and $B \equiv \frac{n}{|\alpha|} - |\alpha|$. N is a normalization factor, $\bar{x}$ and σ are the peak position and width of the Gaussian portion of the function, α is the point at which the function changes to the power function and n is the exponent of the power function. A and B are defined such as to maintain the continuity of the function and it first derivative at α. More details can be found in D. Antreasyan, Crystal Ball Note 321 (1983).

[7] CLEO Collaboration, D. Gibaut *et al.*, Phys. Rev. **53(9)**, 4734-4746 (1996).

[8] M. Bauer *et al.*, Z. Phys. C **34**, 103-115 (1987).

[9] J. Rosner, Phys. Rev. **42(11)**, 3732-3740 (1990).

[10] M. Neubert and V. Rieckert, Nucl. Phys. B **382**, 97-119 (1992)

[11] ARGUS Collaboration, H. Albrecht *et al.*, Z. Phys. C **54**, 1-11 (1992).